

PACS numbers: 52.50.Jm; 33.80.Eh; 42.68.Ay
DOI: 10.1070/QE2011v041n04ABEH014486

Intensity clamping in the filament of femtosecond laser radiation

V.P. Kandidov, V.Yu. Fedorov, O.V. Tverskoy, O.G. Kosareva, S.L. Chin

***Abstract*. We have studied numerically the evolution of the light field intensity and induced refractive index of a medium upon filamentation of femtosecond laser radiation in air. It is shown that the intensity clamping results from the dynamic balance of optical powers of nonlinear lenses, induced by radiation due to the Kerr nonlinearity of air, and laser plasma produced during photoionisation. We have found the relation between the peak values of the light field intensity and the electron density in laser-produced plasma, as well as the transverse sizes of the filament and the plasma channel.**

Keywords: *filamentation, femtosecond pulse, intensity clamping, laser plasma, nonlinear lens, Kerr self-focusing, plasma defocusing.*

1. Introduction

When femtosecond laser radiation propagates in transparent dielectrics, the light field is localised in a narrow extended filament, whose formation is the result of the nonlinear optical interaction of short-duration radiation with a medium [1 – 4]. A filament is a continuous set of nonlinear foci, which are formed due to Kerr self-focusing in temporal slices of the pulse, starting from the slice corresponding to the peak power, and then subsequently in other slices of its leading edge. The region of energy localisation in the nonlinear focus 'flies' forward with the pulse, thereby producing an extended filament. The collapsing growth of the intensity in nonlinear foci is limited by radiation defocusing in the induced laser plasma, which is generated when the intensity exceeds the medium photoionisation threshold. Restriction of the Kerr increase in the laser radiation intensity was first found for a picosecond pulse at optical breakdown in glass [5], and subsequently recorded in laboratory experiments on filamentation of femtosecond laser pulses in air [6 – 8]. However, at atmospheric paths of length of several hundred meters, Mechain et al. [9] failed to register the laser plasma along the entire length of the filament. The dynamic balance of the Kerr self-focusing and plasma defocusing leads to the stability of parameters in the extended filament of a femtosecond pulse. At present, the influence of higher-order nonlinearities of a medium on the limitation of the laser intensity rise in the filament is being discussed [10, 11].

The filament parameters are determined by the nonlinear optical properties of a medium, the wavelength of pulsed laser radiation and its focusing. According to various experimental data, in air at a wavelength of 800 nm the self-focusing critical power $P_{\rm cr} = 2 - 5$ GW, the radius of the filament of a collimated beam $r_{\rm fil} \approx 50$ μm, the radius of the plasma channel $r_{\rm pl} \approx 20$ μm, and the peak intensity $I_{\rm peak} = 10^{13} - 10^{14}$ W cm^{-2} [4]. To evaluate the light field intensity and the electron density, Braun et al. [12] used the Javan – Kelley analysis [13], according to which both the phase shift caused by the Kerr nonlinearity and the phase shift due to diffraction and plasma nonlinearity are equal in magnitude. The maximum light field intensity upon filamentation in air, obtained in [14] from this condition involving the experimental data on the photoionisation rate of nitrogen and oxygen, is 5×10^{13} W cm^{-2}, which is consistent with the results of experiments using a Ti:sapphire laser. However, the fact that the Kerr and plasma refractive index additives on the beam axis of pulsed radiation are equal in magnitude does not mean that the optical powers of nonlinear lenses, focusing and defocusing radiation, also become equal in magnitude. Indeed, the diameter of the plasma channel, in which the refractive index additive is negative, is much smaller than the diameter of the filament, i.e., a region where the refractive index additive is positive [15]. With this ratio of the geometric parameters of the filament, the equality of optical powers of induced nonlinear lenses is possible only when refractive index additives arising from plasma and Kerr nonlinearities on the beam axis of pulsed radiation are significantly different in magnitude [16].

In this paper we study the dependence of the intensity distributions of femtosecond laser radiation as well as of the phase shifts and refractive index additives caused in air by the Kerr nonlinearity and the nonlinearity of the induced laser plasma on distance. It is shown that the saturation of the avalanche growth in the intensity upon self-focusing of the temporal slices of the pulse is determined by the optical power of lenses associated with the Kerr and plasma nonlinearities. Based on the analysis of the optical power of nonlinear optical lenses induced in the medium, we obtain the relation for the geometric parameters of the filament and the plasma channel, as well as for the peak intensity and electron density.

V.P. Kandidov, V.Yu. Fedorov, O.V. Tverskoy, O.G. Kosareva Department of Physics, M.V. Lomonosov Moscow State University, Vorob'evy gory, 119991 Moscow, Russia; e-mail: kandidov@physics.msu.ru;
S.L. Chin Centre d'Optique, Photonique et Laser (COPL) and Département de Physique, de Génie Physique et d'Optique, Université Laval, Québec, Québec G1V0A6, Canada;
e-mail: see.leang.chin@copl.ulaval.ca

Received 10 November 2010; revision received 7 February 2011
Kvantovaya Elektronika **41** (4) 382 – 386 (2011)
Translated by I.A. Ulitkin

2. Optical power of nonlinear lenses

In gases, the refractive index additive $\Delta n_{\rm K}(r,z,t)$ caused by the cubic nonlinearity is determined by the contribution of the electronic component, which can be considered instantaneous for a femtosecond pulse, and the contribution of stimulated Raman scattering on rotational transitions of molecules for which the characteristic response time in air is $\tau_{\rm nl} = 70$ fs [17]. According to [18], for the additive $\Delta n_{\rm K}(r,z,t)$ in air we can use the approximation

$$\Delta n_{\rm K}(r,z,t) = \frac{1}{2}n_2\left[I(r,z,t) + \int H(t-t')I(r,z,t')\mathrm{d}t'\right], \quad (1)$$

where $I(r,z,t)$ is the laser intensity; $H(t)$ is a function of the nonlinear response of air, caused by stimulated scattering; n_2 is the air nonlinearity coefficient determined for pulses with duration $\tau_0 \gg \tau_{\rm nl}$.

The change $\Delta n_{\rm pl}(r,z,t)$ in the refractive index of air, induced by the generation of laser-produced plasma, is determined by the photoionisation process, because the contribution of avalanche ionisation in atmospheric pressure gases is negligible:

$$\Delta n_{\rm pl}(r,z,t) = -\frac{e^2\lambda^2}{8\pi^2 m_{\rm e}\varepsilon_0 c_0^2}N_{\rm e}(r,z,t), \quad (2)$$

where e and $m_{\rm e}$ are the electron charge and mass; ε_0 is the dielectric constant; c_0 is the speed of light; λ is the central wavelength in the spectrum of the pulse. A change in the electron density $N_{\rm e}$ while neglecting recombination and avalanche ionisation in air at atmospheric pressure is described by the kinetic equation

$$\frac{\partial N_{\rm e}(r,z,t)}{\partial t} = R(I)[N_0 - N_{\rm e}(r,z,t)], \quad (3)$$

where $R(I)$ and $N_0 = 10^{19}$ cm^{-3} is the ionisation rate of gas components of air and their concentration.

Upon filamentation of femtosecond radiation, an axisymmetric Townes mode and, therefore, axisymmetric distributions of the induced refractive index additive are formed in the plane of the laser beam cross section. The induced additives $\Delta n_{\rm K}(r,z,t)$ and $\Delta n_{\rm pl}(r,z,t)$ vary with time during the pulse and with the distance z along the pulse propagation direction. Evolution of the intensity profile $I(r,z,t^*)$ in some temporal slice of the pulse ($t = t^*$) with distance is determined by the radial distribution of changes in the phase of the complex amplitude, caused by the Kerr [$\Delta\varphi_{\rm K}(r,z,t^*)$] and plasma [$\Delta\varphi_{\rm pl}(r,z,t^*)$] nonlinearities. As follows from the eikonal equation of the complex amplitude in a nonlinear medium [19], the changes in the phase $\Delta\varphi_{\rm K,pl}(r,z,t^*)$ are proportional to the additives of medium's refractive index $\Delta n_{\rm K,pl}(r,z,t^*)$. Let us represent in the vicinity of the filament axis the radial dependences of the additives $\Delta n_{\rm K}(r,z,t^*)$ and $\Delta n_{\rm pl}(r,z,t^*)$ as series, keeping the first two terms of the expansion:

$$\Delta n_{\rm K}(r,z,t^*) = \Delta n_{\rm K}(r=0,z,t^*) + \frac{1}{2}\frac{\partial^2\Delta n_{\rm K}(r,z,t^*)}{\partial r^2}\bigg|_{r=0} r^2,$$
$$\Delta n_{\rm pl}(r,z,t^*) = \Delta n_{\rm pl}(r=0,z,t^*) + \frac{1}{2}\frac{\partial^2\Delta n_{\rm pl}(r,z,t^*)}{\partial r^2}\bigg|_{r=0} r^2. \quad (4)$$

The first terms in (4) are the refractive index additives on the filament axis which are caused by the Kerr [$\Delta n_{\rm K}(r=0,z,t^*)$] and plasma [$\Delta n_{\rm pl}(r=0,z,t^*)$] nonlinearities. The fact that the absolute values of these terms are equal forms the basis for the analysis carried out in [12, 14] to estimate the peak intensity in the filament. The second term in (4) determines the curvature of the radial distributions of the refractive index additives and, hence, the radiation-induced shifts of the phase of the complex amplitude. Representation (4) corresponds to the parabolic approximation in the theory of propagation of light beams. One can introduce (for some small interval at the length of the pulse propagation Δz) the optical powers of the Kerr [$D_{\rm K}(z,t^*)$] and plasma [$D_{\rm pl}(z,t^*)$] nonlinear lenses:

$$D_{\rm K}(z,t^*) = \frac{\partial^2\Delta n_{\rm K}(r,z,t^*)}{\partial r^2}\bigg|_{r=0}\Delta z,$$
$$D_{\rm pl}(z,t^*) = \frac{\partial^2\Delta n_{\rm pl}(r,z,t^*)}{\partial r^2}\bigg|_{r=0}\Delta z. \quad (5)$$

The relation between the optical powers of nonlinear lenses induced by laser radiation in the medium determines the evolution of the intensity distribution in the temporal slice t^* of the pulse.

3. Spatial distributions of the laser radiation intensity and the induced changes in the refractive index

To analyse the evolution of the light field intensity and the refractive index additives of the Kerr [$\Delta n_{\rm K}(r,z,t)$] and plasma [$\Delta n_{\rm pl}(r,z,t)$] nonlinearities, we solved numerically the self-consistent nonstationary problem of femtosecond laser radiation filamentation in air, which includes expressions (1)–(3) and the equation for the pulse envelope $E(r,z,t)$ in the moving coordinate system

$$2{\rm i}k_0\frac{\partial E(r,z,t)}{\partial z} = \Delta_\perp E(r,z,t) + k_0k_2\frac{\partial^2 E(r,z,t)}{\partial t^2}$$
$$+ 2k_0^2[\Delta n_{\rm K}(r,z,t) + \Delta n_{\rm pl}(r,z,t)]E(r,z,t) + {\rm i}\alpha E(r,z,t), \quad (6)$$

where $k_0 = 2\pi/\lambda$. The first and third terms on the right-hand side of (6) describe the 'pulse diffraction' and nonlinear changes in the envelope phase, the second term with the coefficient $k_2 = \partial^2 k_0/\partial\omega^2$ – the group-velocity dispersion, and the last term with the coefficient α – a decrease in the amplitude during the photoionisation of air. Equation (6) does not take into account higher orders of the theory of dispersion. We consider collimated radiation with a Gaussian distribution of the field amplitude in space and time:

$$E(r,z=0,t) = E_0\exp[-r^2/(2a_0^2)]\exp[-t^2/(2\tau_0^2)]. \quad (7)$$

As an example, we present below the results of simulations for the central temporal slice ($t = 0$) of the pulse at a wavelength of 800 nm with an energy $W = 2.6$ mJ, peak power $P_{\rm peak} = 14.5$ GW and the distribution parameters $a_0 = 1.2$ mm, $\tau_0 = 100$ fs. Pulses with close parameters are used in laboratory experiments on filamentation of radiation in air. Figure 1 shows the spatial intensity distributions $I(r)|_{t=0}$ and phase shifts caused by the Kerr [$\Delta\varphi_{\rm K}(r)|_{t=0}$] and

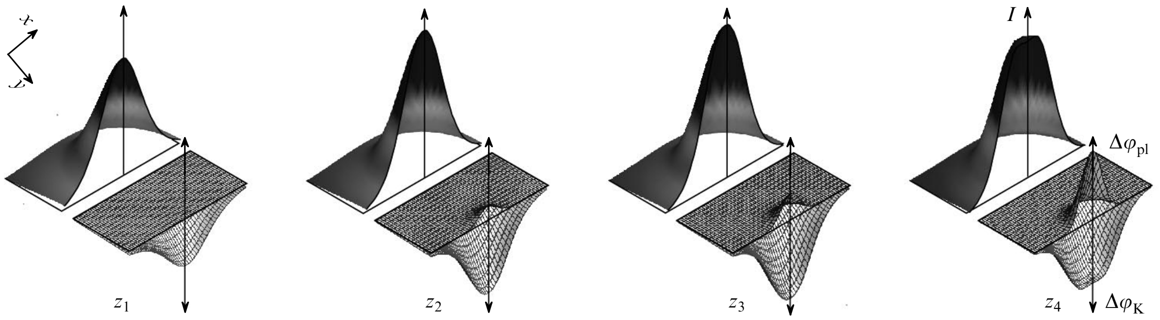

Figure 1. Intensity distributions $I(r)|_{t=0}$ (top row), as well as nonlinear phase shifts due to the Kerr $[\Delta\varphi_{\rm K}(r)]$ and plasma $[\Delta\varphi_{\rm pl}(r)]$ nonlinearities (bottom row) for the central temporal slice of the pulse ($t = 0$) at some distances z in the vicinity of the filament onset in the air, shown in half plane perpendicular to the direction of radiation propagation. The pulse parameters are given in the text.

plasma $[\Delta\varphi_{\rm pl}(r)|_{t=0}]$ nonlinearities plotted for some distances z in the vicinity of the filament onset in a plane perpendicular to the propagation direction. The radial distributions of the Kerr refractive index additive $\Delta n_{\rm K}(r)$ in the medium and of the pulse intensity $I(r)$ are similar. At a distance $z = z_1$ the additive $\Delta n_{\rm K}(r)$ is positive, and the nonlinear phase in the paraxial region of the pulse is negative ($\Delta\varphi_{\rm K} < 0$), which corresponds to a lens with positive optical power $[D_{\rm K}(z_1) > 0]$ focusing radiation.

Then, the intensity grows and the electron density increases in the laser plasma whose negative contribution to the refractive index additive $[\Delta n_{\rm pl}(r) < 0]$ becomes noticeable at $z = z_2$. This causes a positive shift of the nonlinear phase ($\Delta\varphi_{\rm pl} > 0$) and, as a result, the emergence of a lens with negative optical power $[D_{\rm pl}(z_2) < 0]$ on the filament axis. The plasma lens aperture size is determined by the diameter of the plasma channel, which is smaller than the filament diameter determining the Kerr lens aperture. Therefore, the intensity on the filament axis increases due to 'radiation flow' from the periphery of the cross section of the beam, which is being focused by a wide-aperture Kerr lens.

At a distance $z = z_3$, the pulse intensity stops growing. However, the absolute values of the refractive index additive and, hence, the phase shift, caused by the Kerr nonlinearity, are significantly larger than those due to the plasma nonlinearity: $|\Delta n_{\rm K}(r)| \gg |\Delta n_{\rm pl}(r)|$ and $|\Delta\varphi_{\rm K}| \gg |\Delta\varphi_{\rm pl}|$. At a distance $z = z_4$, on the axis ($r = 0$) the absolute values of the refractive index additives and phase shifts, caused by the Kerr and plasma nonlinearities, are equal: $|\Delta n_{\rm K}(r = 0)| = |\Delta n_{\rm pl}(r = 0)|$ and $|\Delta\varphi_{\rm K}(r = 0)| = |\Delta\varphi_{\rm pl}(r = 0)|$. In this case, the intensity is smaller than the peak value achieved at $z \approx z_3$.

4. Evolution of the parameters of the filament and optical power of nonlinear lenses

Figure 2a illustrates the change in the axial intensity $I(z)|_{r=0}$ and electron density $N_{\rm e}(z)|_{r=0}$ for the central temporal slice ($t = 0$) of the pulse under study with distance. Figure 2b presents the refractive index additives due to the Kerr $[\Delta n_{\rm K}(z)|_{r=0}]$ and plasma $[\Delta n_{\rm pl}(z)|_{r=0}]$ nonlinearities, and their sum $[\Delta n_{\rm K}(z) + \Delta n_{\rm pl}(z)]|_{r=0}$. Figure 2c shows the optical power of the Kerr $[D_{\rm K}(z)]$ and plasma $[D_{\rm pl}(z)]$ nonlinear lenses as well as their sum versus distance. Up to a distance $z = z_1$, the density of electrons on the axis is four orders of magnitude smaller than that of neutral molecules ($N_0 \approx 10^{19}$ cm^{-3}), the refractive index additive $\Delta n_{\rm pl}(z)|_{r=0}$ and optical power of the lens $D_{\rm pl}(z)$, formed by the plasma, are close to zero and do not affect the collapsing growth of the pulse intensity caused by the Kerr nonlinearity, for which the $\Delta n_{\rm K}(z)|_{r=0} > 0$ and $D_{\rm K}(z) > 0$. At $z_2 \approx 3.41$ m, the electron density on the axis increases to $\sim 10^{16}$ cm^{-3}

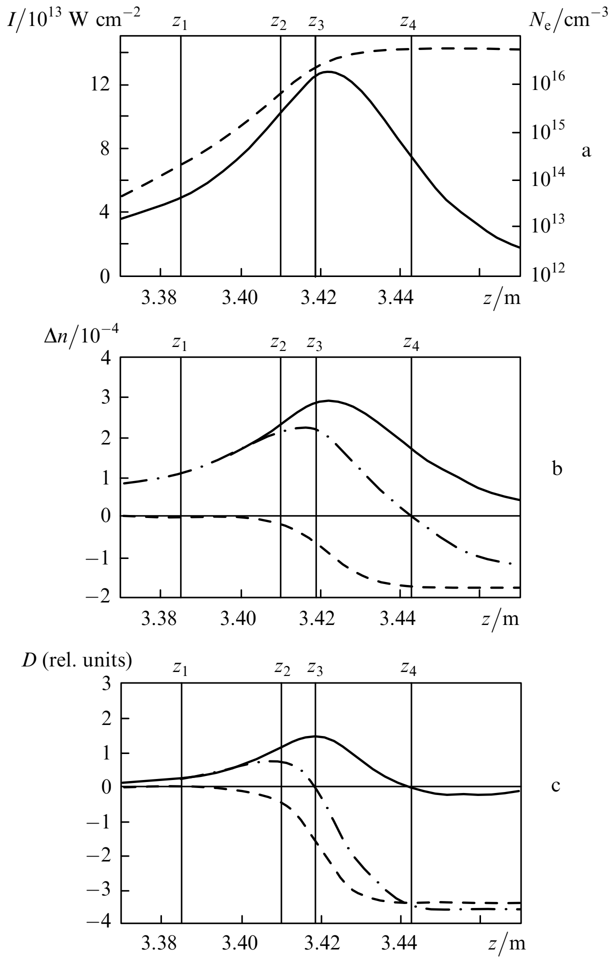

Figure 2. Dependences of axial intensities $I(z)|_{r=0}$ (solid curve) and electron densities $N_{\rm e}(z)|_{r=0}$ (dashed curve) in the central temporal slice of the pulse ($t = 0$) in the vicinity of the filament onset (a), of the Kerr $[\Delta n_{\rm K}(z)|_{r=0}]$ (solid line) and plasma $[\Delta n_{\rm pl}(z)|_{r=0}]$ (dashed curve) refractive index additives and their sum (dot-dashed curve) in air (b), and of the optical powers of the Kerr $[D_{\rm K}(z)]$ (solid curve) and plasma $[D_{\rm pl}(z)]$ (dashed curve) lenses and their sum (dash-and-dot curve) (c) on the distance z. Pulse parameters are the same as in Fig. 1.

(Fig. 2a), the plasma refractive index additive is much smaller in magnitude than the Kerr additive ($|\Delta n_{\rm pl}| \ll |\Delta n_{\rm K}|$) (Fig. 2b). However, the absolute values of the optical powers of the plasma ($|D_{\rm pl}|$) and Kerr ($|D_{\rm K}|$) lenses are comparable, which stops a further increase in the total focusing power with distance (Fig. 2c). This leads to slower avalanche growth of the intensity on the axis, which is characteristic of the laser beam self-focusing.

The light field intensity is clamped in the filament when the optical powers of the Kerr and plasma lenses are equal in magnitude:

$$|D_{\rm K}(z_3)| = |D_{\rm pl}(z_3)|. \tag{8}$$

For the pulse under study, the intensity at $z_3 \approx 3.42$ m is equal with a high accuracy to the peak intensity $I_{\rm peak}$ in the filament (Fig. 2a). A slight difference of z_3 from the distance where the intensity clamping found from equation (6) actually occurs, is due to an error of axial aberration-free approximation (4). The absolute values of axial refractive index additives caused by the Kerr and plasma nonlinearities become equal at $z = z_4$, when the intensity is approximately one and a half times smaller than the peak intensity (Figs 2a, b). At $z = z_4$, the optical power of the Kerr lens is close to zero and the net effect of the nonlinearities is reduced to plasma defocusing (Fig. 2c), which results in the formation of a ring in the intensity distribution (Fig. 1). With a decrease in the intensity at $z > z_4$, the ionisation rate, for which the estimate $R(I) \sim I^K$ is valid, drastically decreases, where K is the multiphotonity order equal to 8 for oxygen molecules and 11 for nitrogen molecules.

Figure 3 demonstrates the effect of the scales of the spatial distribution of the induced refractive index additives on the optical power of the nonlinear lens. The plasma channel diameter is approximately half the filament diameter, within which the Kerr nonlinearity is induced. Therefore, the plasma produces a lens whose optical power is equal in magnitude to the optical power of the Kerr lens at the axial refractive index additive $\Delta n_{\rm pl}|_{r=0}$, which is half $\Delta n_{\rm K}|_{r=0}$ (Fig. 3a). When the axial refractive index additives are equal in magnitude, the scale of the spatial distribution of the Kerr additive $|\Delta n_{\rm K}(r)|$ is much larger than that of the plasma additive $|\Delta n_{\rm pl}(r)|$, and the optical power of the Kerr lens is much smaller than that of the plasma one (Fig. 3b).

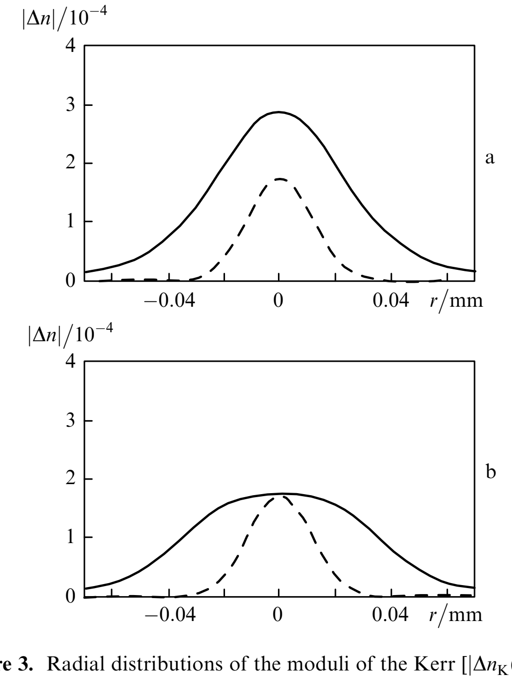

Figure 3. Radial distributions of the moduli of the Kerr [$|\Delta n_{\rm K}(r)|$] (solid curves) and plasma [$|\Delta n_{\rm pl}(r)|$] (dashed curves) refractive index additives in the central temporal slice of the pulse ($t = 0$) for distances where optical powers of nonlinear lenses (a) and additives on the axis ($r = 0$) (b) are equal.

The numerical experiments have shown that the obtained regularities hold true for different temporal slices at the leading and trailing edges of the pulses at different radiation wavelengths.

5. Modified Javan – Kelley analysis

At a distance, where the optical powers of nonlinear lenses are equal in magnitude, the intensity of the light field on the beam axis of pulsed radiation almost coincides with the peak intensity $I_{\rm peak,}$ and the electron density in the induced plasma is close to the maximum value $N_{\rm e\,peak}$ (Fig. 2a). This allows one to obtain from condition (8) an analytical relation between the peak values of the intensity and the electron density on the axis as well as between the transverse sizes of the filament and plasma channel.

Let us approximate in the vicinity of the axis the radial distributions of the intensity $I(r)$ and the electron density $N_{\rm e}(r)$ by the Gaussian functions:

$$I(r) = I_{\rm peak}\exp(-r^2/r_{\rm int}^2),$$
$$N_{\rm e}(r) = N_{\rm e\,peak}\exp(-r^2/r_{\rm pl}^2). \tag{9}$$

In the experiments, the filament radius $r_{\rm fil}$ is determined by the distribution of the surface energy density in the filament cross section $F(r,z)$, measured at a distance z:

$$F(r,z) = \int I(r,z,t)\mathrm{d}t. \tag{10}$$

Because in the vicinity of the filament axis the main contribution to the distribution $F(r,z)$ is made by a temporal slice where the intensity is maximal, we can assume that

$$r_{\rm fil} \approx r_{\rm int}. \tag{11}$$

The parameter $r_{\rm pl}$ in (9) is equal to the radius of the plasma channel.

We assume that the pulse duration is large enough and the delay of the response of the cubic nonlinearity of air can be neglected. Then, expression (1) takes the form

$$\Delta n_{\rm K}(r,z,t) = n_2 I(r,z,t). \tag{12}$$

Substituting (2) and (12) into (5), using approximation (9) and approximation (11), we obtain from (8) the relationship:

$$n_2\frac{I_{\rm peak}}{r_{\rm fil}^2} = \frac{e^2\lambda^2}{8\pi^2\varepsilon_0 m_{\rm e}c_0^2}\frac{N_{\rm e\,peak}}{r_{\rm pl}^2}. \tag{13}$$

This relationship makes it possible to estimate one of the unknown filament parameters, to identify tendencies for changes in the peak intensities $I_{\rm peak}$and the electron density $N_{\rm e\,peak}$, as well as the radii $r_{\rm fill}$ and $r_{\rm pl}$ by varying the radiation wavelengths. According to the results of computer simulations performed for laser pulses with wavelengths 0.4 – 1.24 μm, the accuracy of estimates (13) is relatively small. The ratio of the radii of the filament and the plasma channel $r_{\rm fil}/r_{\rm pl}$, estimated by (13), is approximately twice the value obtained in the computer simulations when determining $r_{\rm fill}$ by the profile of the surface energy density in the filament cross section.

6. Conclusions

The intensity clamping in the femtosecond laser filament results from the dynamic balance of optical powers of lenses induced by laser radiation: a focusing lens, which is due to the Kerr nonlinearity of the medium, and a defocusing lens, which is produced by the laser plasma. During the pulse propagation the avalanche increase in the intensity in its temporal slices, caused by the Kerr nonlinearity, is replaced by its slow increase at a distance, where the growth of the total focusing power of nonlinear lenses stops upon the emergence of the laser plasma. The intensity is clamped and reaches a peak value in the filament if the optical powers of lenses associated with the Kerr and plasma nonlinearities rather than absolute refractive index additives caused by these nonlinearities are equal in magnitude. From the condition of the balance of optical powers of nonlinear lenses induced by radiation we can estimate the relation between the peak values of the intensity and electron density as well as between the transverse sizes of the filament and plasma channel.

The considered scenario of intensity clamping is generalised to terrawatt pulses, which form a beam consisting of a random set of interacting filaments and plasma channels [20].

Acknowledgements. V.P. Kandidov acknowledges the support of the Russian Foundation for Basic Research (Grant No. 08-02-00517a).

References

1. Chin S.L., Hosseini S.A., Liu W., Luo Q., Theberge F., Akozbek N., Becker A., Kandidov V., Kosareva O., Schroeder H. *Can. J. Phys.*, **83**, 863 (2005).
2. Couairon A., Mysyrowicz A. *Phys. Rep.*, **441**, 47 (2007).
3. Berge L., Skupin S., Nuter R., Kasparian J., Wolf J.-P. *Rep. Prog. Phys.*, **70**, 1633 (2007).
4. Kandidov V.P., Shlenov S.A., Kosareva O.G. *Kvantovaya Electron.*, 39, 205 (2009) [*Quantum Electron.*, **39**, 205 (2009)].
5. Yablonovich E., Bloembergen N. *Phys. Rev. Lett.*, **29**, 907 (1972).
6. Tzortzakis S., Franco M.A., Andre Y.-B., Chiron A., Lamouroux B., Prade B.S., Mysyrowicz A. *Phys. Rev. E*, **60**, 3505 (1999).
7. Schillinger H., Sauerbrey R. *Appl. Phys. B*, **68**, 753 (1999).
8. Talebpour A., Abdel-Fattah M., Chin S.L. *Opt. Commun.*, **183**, 479 (2000).
9. Mechain G., Couairon A., Andre Y.-B., D'Amico C., et al. *Appl. Phys. B*, **79**, 379 (2004).
10. Béjot P., Kasparian J., Henin S., Loriot V., Vieillard T., Hertz E., Faucher O., Lavorel B., Wolf J.-P. *Phys. Rev. Lett.*, **104**, 103903 (2010) .
11. Kolesik M., Wright E.M., Moloney J.V. *Opt. Lett.*, **35**, 2550 (2010).
12. Braun A., Korn G., Liu X., Du D., Squier J., Mourou G. *Opt. Lett.*, **20**, 73 (1995).
13. Javan A., Kelley P. *IEEE J. Quantum Electron.*, **2** (9), 470 (1966).
14. Kasparian J., Sauerbrey R., Chin S.L. *Appl. Phys. B*, **71**, 877 (2000).
15. Jiansheng Liu, Zuoliang Duan, Zhinan Zeng, Xinhua Xie, Yunpei Deng, Ruxin Li, Zhizhan Xu, Chin S.L. *Phys. Rev. E*, **72**, 026412 (2005).
16. Fedorov V.Yu., Kandidov V.P., Kosareva O.G., Tverskoy O.V., Chin S.L. *Book of Abstracts. COFIL'2010* (Crete, Greece, 2010) p. 107.
17. Oleinikov P.A., Platonenko V.T. *Laser Phys.*, **3**, 618 (1993).
18. Mlejnek M., Wright E.M., Moloney J.V. *Opt. Lett.*, **23**, 382 (1998).
19. Vinogradova M.B., Rudenko O.V., Sukhorukov A.P. *Teoriya voln* (Wave Theory) (Moscow: Nauka, 1990).
20. Kandidov V.P., Shlenov S.A., in *Glubokoe kanalirovanie i filamentatsiya moshchnogo izlucheniya v veshchestve* (Deep Channeling and Filamentation of Intense Laser Radiation in Matter) (Moscow: Interkontakt Nauka, 2009) Part 2, pp 185 – 266.